HAL open science

State estimation in alcoholic fermentation models: a case-study in wine-making conditions

Martin Fleurial, Ludovic Sacchelli, Agustín G Yabo

To cite this version:

Martin Fleurial, Ludovic Sacchelli, Agustín G Yabo. State estimation in alcoholic fermentation models: a case-study in wine-making conditions. 2024 European Control Conference (ECC), Jun 2024, Stockholm, Sweden. pp.412-417, 10.23919/ECC64448.2024.10591226 . hal-04269299v3

HAL Id: hal-04269299

https://hal.science/hal-04269299v3

Submitted on 27 Mar 2024

HAL is a multi-disciplinary open access archive for the deposit and dissemination of scientific research documents, whether they are published or not. The documents may come from teaching and research institutions in France or abroad, or from public or private research centers.

L'archive ouverte pluridisciplinaire **HAL**, est destinée au dépôt et à la diffusion de documents scientifiques de niveau recherche, publiés ou non, émanant des établissements d'enseignement et de recherche français ou étrangers, des laboratoires publics ou privés.

State estimation in alcoholic fermentation models: a case-study in wine-making conditions

Martin Fleurial[1], Ludovic Sacchelli[2] and Agustín G. Yabo[3]

***Abstract*— We study the problem of online state estimation during wine fermentation. This problem becomes relevant when trying to control the alcoholic fermentation process with a control law relying on our capacity to estimate the full state, but with partial measurements of the system (which is the case in an industrial framework). We focus on studying observability properties of an alcoholic fermentation model in wine-making conditions. We implement an algorithm of state estimation based on optimality principles on expanding time windows (Full Information Estimator). In order to test the developed algorithms, we compare the results obtained on simulated data as well as experimental data obtained in wine fermentations performed at a laboratory scale.**

I. Introduction

Triggered by the increasing environmental issues, the agri-food industry is undergoing a major transformation towards sustainable practices. In particular, newer concerns are increasingly becoming relevant for the wine industry, related to the energy consumption of the process, or the reduction of the carbon footprint. The latter not only can contribute to a more sustainable industry—and simultaneously reduce production costs—but also complies with the demands of a major niche of the population that is becoming increasingly engaged with ethical and environmental issues [1]. On the other hand, in the current highly competitive market, it is critical to preserve (and potentially improve) the character and quality of wines during the transition to an eco-friendly food industry. These issues are beyond the reach of current enological practices, and represent a challenge for the engineering community. In this context, optimization and control theory become a key tool for their capacity to interfere and drive in real time the fermentation process.

A fundamental starting point in the design and implementation of closed-loop control schemes is an accurate model of wine fermentation. There have been numerous attempts to develop mechanistic models of enological fermentation by considering only the main macrochemical reactions. In this work, we focus on the one proposed in [2] which, despite its simplicity, is able to capture numerous physiological phenomena such as yeast growth on nitrogen, sugar transport, ethanol inhibition and the effect of temperature on synthesis rates. While newer models of wine fermentation have been introduced in recent years, the model proposed in Malherbe *et. al.* meet the requirements for this first work.

A closed-loop approach to regulating winemaking fermentation strongly relies on our capacity to measure and estimate the main variables involved in the process [3], [4]. This happens to be a non-trivial task in alcoholic fermentation due to the nonlinearity of the mathematical models, the strong interdependence of the variables, and the unavailability of industrial-scaled sensors capable of measuring them. For these reasons, it is worthwhile to investigate ad-hoc solutions to the state estimation problem that take into account the specificities of industrial oenological conditions.

Another inherent feature of wine fermentation is the low frequency of the measuring-estimation-control loop, mainly due to the slowness of the fermentation process. This characteristic relaxes a major constraint of regular real-time implementations: the execution time of the algorithm. Thus, on top of other more classical approaches, this opens up the possibility to explore optimality-based estimation algorithms [5], [6], often disregarded for their slow execution times. As an example of alternative approaches, Extended Kalman Filters have been already used in wine fermentation [7]. However, since the approach relies on a linearization of the system, the estimator can diverge if the initial estimate of the state is too far from the real state. Other algorithms that do not rely on mechanistic models of the fermentation process, such as non-parametric Gaussian trackers [8], have proved their efficacy, but can fail to capture the constraints and nonlinearities of the real system.

In this work, we investigate the problem of online state estimation during wine fermentation. In Section II, we present a simple wine fermentation model from the literature [2]. In Section III, we study its observability properties, we propose a partially initialized model adapted to our setting, and we introduce the optimality-based estimation scheme used: the FIE (Full Information Estimator). In Section IV, results using numerical and experimental data from Malherbe et al. are showed. Two optimization methods are tested and compared for the implementation: interior point method, and particle swarm optimization. Finally, we briefly discuss the obtained results.

II. Dynamical models of wine fermentation

A. Dynamical model

The model represents a fermentation process carried out by the yeast *Saccharomyces cerevisiae* developed in [2], and

*This research project was funded by the French National Research Agency (ANR) under the grant agreement STARWINE (ANR-18-CE10-0013).

[1]Martin Fleurial is with Sapienza Università di Roma, Department of Mathematics Guido Castelnuovo, Rome, Italy. martin.fleurial@uniroma1.it

[2]Ludovic Sacchelli is with Université Côte d'Azur, Inria, CNRS, LJAD, France. ludovic.sacchelli@inria.fr

[3]Agustín G. Yabo is with MISTEA, Université Montpellier, INRAE, Institut Agro, Montpellier, France. agustin.yabo@inrae.fr

describes the kinetics of the two main metabolic pathways involved in wine fermentation: 1) the consumption of assimilable nitrogen N and conversion into biomass X, and 2) the production of ethanol E and CO_2 from glucose S. In the model, time t is assumed to be measured in hours; substrate concentration S, ethanol concentration E and assimilable nitrogen concentration N in g.L^{-1}, and biomass X in L^{-1}. The temperature is denoted by T in °C. Substrate consumption by each yeast cell is modeled as proportional to the number of glucose transporters per cell N_{ST}, and their ethanol-inhibited glucose transporter activity ν_{ST}, so that

$$\frac{dS}{dt} = -XN_{ST}(N_0 - N, X, T)\nu_{ST}(S, E, T), \qquad (1)$$

where N_0 denotes the initial concentration of nitrogen. Likewise, nitrogen is assimilated through an ethanol-inhibited absorption mechanism

$$\frac{dN}{dt} = -X\nu_N(N, E, T). \qquad (2)$$

The yeast population is modeled as following a logistic growth where maximal population is induced by the initial assimilable nitrogen N_0

$$\frac{dX}{dt} = k_1(T)X\left[1 - \frac{X}{X_{\max}(N_0)}\right]. \qquad (3)$$

Ethanol is produced in proportion to substrate consumption so that

$$\frac{dE}{dt} = -\mu\frac{dS}{dt} \qquad (4)$$

with $\mu = 1/2.17$. The ethanol-inhibited models are, for glucose transporter activity,

$$\nu_{ST}(S, E, T) = \frac{k_2(T)S}{K_S + S(1 + K_{Si}E^{\alpha_S})},$$

and for the absorption mechanism,

$$\nu_N(N, E, T) = \frac{k_3(T)N}{K_S + N(1 + K_{Ni}E_N^{\alpha})}.$$

Finally, the number of glucose transporters per cell is modeled such that

$$k_2(T)XN_{ST}(\Delta N, X, T) = (\lambda_a + \lambda_c T)\Delta N + (\lambda_b T + \lambda_d)X,$$

and $X_{\max}(N_0) = -10^9(649N_0^2 + 698N_0 + 7)$. Equations (1)-(2)-(3)-(4), with nonnegative initial conditions, constitute the Malherbe et al. wine fermentation model introduced in [2]. See Figure 1 for a simulation. Temperature dependant parameters k_1, k_2, k_3, as well as $\lambda_a, \lambda_b, \lambda_c, \lambda_d$, K_S, K_{Si}, α_S, K_N, K_{Ni}, α_N, and their values[1] are discussed in Malherbe et al.

[1] $\lambda_a = 335, \lambda_b = 0.061, \lambda_c = 3, \lambda_d = -1$, $K_S = 15, K_{Si} = 0.012, \alpha_S = 1.25$, $K_N = 0.03, K_{Ni} = 0.035$, $\alpha_N = 1.5$, $k_1(T) = 0.0287T - 0.3762$, $k_2(T) = 0.035$, $k_3(T) = 0.001$.

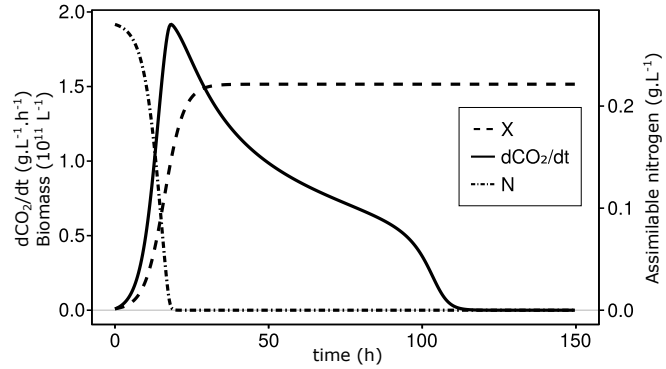

Fig. 1. Example of a trajectory of the dynamical model. Initial state $S_0 = 202$ g.L^{-1}, $N_0 = 0.280$ g.L^{-1}, $X_0 = 1 \cdot 10^9$ L^{-1}, $T = 24$°C.

B. Experimental data

The model was originally calibrated using measurements of cell population of yeasts (X), assimilable nitrogen (N), and CO_2 release. Cell population is measured using an electronic particle counter device, while nitrogen is calculated as the difference between the measurements of total nitrogen and ammonium in the must. These methods require sampling at a certain frequency throughout the fermentation process, and posterior manual analysis of the sample performed by an operator, a procedure quite standard in a laboratory setting, but rather uncommon at an industrial scale. However, CO_2 production rate can be easily computed from weight loss of the must, which gives a precise measurement of CO_2 release [9]. In order to emulate real-time conditions, we consider that only the measurements of CO_2 production rate are accessible, and we base the observability analysis on this hypothesis.

III. State estimation

A. Model discussion in regard to estimation

We consider the problem of state estimation using the more easily available measurement, that is of CO_2 production. The bioprocess is assumed to start from an initial condition $CO_2(0) = E(0) = 0$. As the main chemical reaction in alcoholic fermentation yields an equal amount of ethanol and carbon dioxide per unit of glucose, this implies $CO_2(t) = E(t), \forall t \geq 0$, and so CO_2 measurements are equivalent to measuring E. Thus, we assume that we have access to the output $y = E$ and we wish to provide an estimate of the unknown initial state $(S(0), N(0), X(0))$. We now discuss the model in regard to that particular goal, as well as two reductions adapted to more specific scenarios.

1) Malherbe et al. model: We discuss the dynamical model (1)-(4) with measurement $y = E$ and unknown

$$(S(0), N(0), X(0)) = (S_0, N_0, X_0).$$

The construction of the model defines $X_{\max}(N_0)$ as a degree 2 polynomial in N_0 with two distinct real roots $N_0^- < N_0^+$, such that $X_{\max} > 0$ on (N_0^-, N_0^+). The roots are such that $-0.1 < N_0^- < 0$ and $1 < N_0^+ < 1.1$. For simplification

purposes, we impose $N_0 \in [0,1]$. We define the set of suitable initial conditions

$$\Omega_0 = \{(S_0, N_0, X_0) : 0 \leq S_0, 0 \leq N_0 \leq 1, \\ 0 \leq X_0 \leq X_{\max}(N_0)\}.$$

Proposition 1: Under isothermal conditions (T constant), for any $0 \leq t_1 < t_2$, System (1)-(4) is observable over $[t_1, t_2]$. That is, for any two trajectories of (1)-(4) with initial conditions such that $(S_0, N_0, X_0,), (\tilde{S}_0, \tilde{N}_0, \tilde{X}_0) \in \Omega$, $E_{|[t_1,t_2]} \equiv \tilde{E}_{|[t_1,t_2]}$ implies $(S_0, N_0, X_0) = (\tilde{S}_0, \tilde{N}_0, \tilde{X}_0)$.

Proof is found in Appendix I. The proposition can be extended to include some sufficiently general non-isothermal conditions. However, this extension is quite intricate (but not challenging) and falls out of the scope of this paper.

2) Partially initialized model: The above problem can be refined for estimation purposes in the particular case where a measurement of the initial substrate concentration was experimentally obtained. This is sometimes the case in the experimental setting described in sections I and II-B. Under these assumptions, it may be more reasonable to not use the same estimation method.However, the initial measurement may be biased, so we propose a new formulation of the estimation problem with bias that shares its observability properties with the original problem.

We denote the initial (biased) measurement with $S_0^{\exp}$, and we linearize the system around the trajectory that has $S_0 = S_0^{\exp}$, so that we still have $\frac{dE}{dt} = -\mu \frac{dS}{dt}$, but we assume $S = S^{\exp} + S^{\text{lin}}$, with $\Delta N = N_0 - N$

$$\frac{dS^{\exp}}{dt} = -XN_{ST}(\Delta N, X, T)\nu_{ST}(S^{\exp}, E, T) \quad (5)$$

$$\frac{dS^{\text{lin}}}{dt} = -XN_{ST}(\Delta N, X, T)\partial_S \nu_{ST}(S^{\exp}, E, T)S^{\text{lin}}. \quad (6)$$

Under this assumption, the unknown S_0 is replaced with S_0^{lin}. Proposition 1 holds with $S = S^{\exp} + S^{\text{lin}}$.

Proposition 2: Under isothermal conditions, for any $0 \leq t_1 < t_2$, System (5)-(6)-(2)-(4) is observable over $[t_1, t_2]$. That is, for any two trajectories of (5)-(6)-(2)-(4) with initial conditions such that $(S_0^{\exp} + S_0^{\text{lin}}, N_0, X_0,), (S_0^{\exp} + \tilde{S}_0^{\text{lin}}, \tilde{N}_0, \tilde{X}_0) \in \Omega$, $E_{|[t_1,t_2]} \equiv \tilde{E}_{|[t_1,t_2]}$ implies $(S_0^{\text{lin}}, N_0, X_0) = (\tilde{S}_0^{\text{lin}}, \tilde{N}_0, \tilde{X}_0)$.
The proof can be found in Appendix I.

Behavior of the solutions of this system near the tail end of the reaction do not agree with the biological setting ($S^{\exp} + S^{\text{lin}}$ can have positive derivative for a short period of time near the end of the reaction, see Figure 2). This is not an issue for the estimation problem at hand, where we focus on the beginning of the reaction for control purposes. For what regards the dynamical model for the last part of the reaction, when both N and X are stabilized. We can use another simplified model.

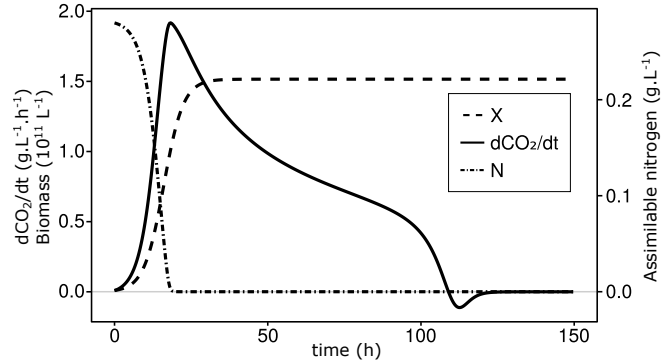

Fig. 2. Example of a trajectory of the partially linearized model. Initial state $S_0^{\exp} = 212$ g.L^{-1}, $S_0^{\text{lin}} = -10$ g.L^{-1}, $N_0 = 0.280$ g.L^{-1} and $X_0 = 1 \cdot 10^9$ L^{-1}, $T = 24°$C. The value of S_0^{lin} has been voluntarily picked large to highlight the difference in the trajectories near the end of the reaction.

3) Tail end model: Study of the trajectories of System (1)-(4) (see Figure 1, for instance) reveal that, under the assumptions of the Malherbe et al. model, both nitrogen N and biomass X reach their equilibria, $N_f = 0$, $X_f = X_{\max}(N_0)$, relatively early in the overall fermentation process (at least if we consider the batch case, without nitrogen introduction). The necessary time to reach these equilibria is of the order of twice the time to peak of $\frac{dCO_2}{dt}$, around the 40 to 60 hour mark in our case. For this reason, we mention an alternative linearized model and briefly discuss its properties, but we do not present further experiments on the model, as we wish to focus on earlier parts of the fermentation. We denote by $N_{ST}(N_0, X_f, T) = N_{STf}$, and we assume that at $t = t^*$, $N = N_f = 0$, $X = X_f$ are valid approximations, so that

$$\begin{aligned} \frac{dS}{dt} &= -X_f N_{STf} \nu_{ST}(S, E, T) \\ \frac{dE}{dt} &= -\mu \frac{dS}{dt} \\ y &= E. \end{aligned} \quad (7)$$

Now, the set of unknowns to estimate is divided between the initial state $S_* = S(t^*)$ and the unknown parameter $X_f N_{STf} = X_{\max}(N_0) N_{ST}(N_0, X_{\max}(N_0), T)$.

Proposition 3: Under isothermal conditions, for any $t^* \leq t_1 < t_2$, System 7 is observable in the sense that for any $S_*, \tilde{S}_* \geq 0$ $N_0, \tilde{N}_0 \in [0,1]$, $E_{|[t_1,t_2]} \equiv \tilde{E}_{|[t_1,t_2]}$ implies $(S_*, N_0) = (\tilde{S}_*, \tilde{N}_0)$.
The proof can be deduced from the previous two and is left as an exercise to the reader.

B. Estimation method

The long duration of the wine fermentation reaction allows considering offline estimation methods for the online estimation and control of the process. For instance, in the experimental setting described previously, a measurement of emitted CO_2 is taken every 30 minutes. For this reason, optimization-based methods appear to be well suited for the estimation problem at hand. In particular, we consider MHE (Moving Horizon Estimation), the estimation side of

model predictive control [10], [6]. In particular, we consider a subclass of MHE, known as FIE (Full Information Estimation), which consists of minimizing the least squares energy over the time interval $[0, T_k]$ at each measurement time T_k. For that, let us rewrite (1)-(4) as $\frac{d\xi}{dt} = f(\xi)$, with $\xi = (S, N, X, E)$. For a given trajectory $\xi(\cdot)$, we assume knowledge of a measurement function $\mathbf{y} = E + v$, where v is a measurement noise, that we assume to be of class $L^2(\mathbb{R})$. See Figure 3 for one such experimental situation. For any initial condition $\xi_0 \in \Omega_0' := \Omega_0 \times \{0\}$, we can define $t \mapsto y_{\xi_0}(t)$ the model predicted output. For an increasing sequence of time horizons $T_k > 0$, the moving horizon estimate over $[0, T_k]$ is for us the trajectory $\hat{\xi}^k$ such that $\hat{\xi}^k(0)$ solves

$$\begin{aligned} \underset{\xi_0 \in \Omega_0'}{\operatorname{argmin}}\ J_k(\xi_0) :=& \alpha |\hat{\xi}^{k-1}(0) - \xi_0|^2 \\ &+ \int_0^{T_k} |\mathbf{y}(s) - y_{\xi_0}(s)|^2\, ds. \end{aligned} \tag{8}$$

The quantity $\alpha \geq 0$ is a weighted memory term that can be set to 0.

Remark 4: In full generality, process noise should be accounted for in such problems. They are left for a later study at the moment.

In that context, observability of (1)-(4) with output $y = E$ yields a soft convergence result. The statement itself is a reformulation of the classical MHE globally asymptotically stable convergence theorems (such as the ones found in [5], [6]), se we do not re-prove it.

Proposition 5: Under the above assumptions, there exists a $\mathcal{K}$-class function ω such that

$$|\xi(t) - \hat{\xi}^k(t)| \leq \omega(\|v\|_{L^2(0,T_k)}), \quad \forall t \in [0, T_k]$$

In particular, $\xi = \hat{\xi}^k$ on $[0, T_k]$ if $v = 0$. Furthermore, if $\|v\|_{L^2(T_k,+\infty)} \to 0$ as $k \to 0$, then $\hat{\xi}^k(0) \to \xi_0$.

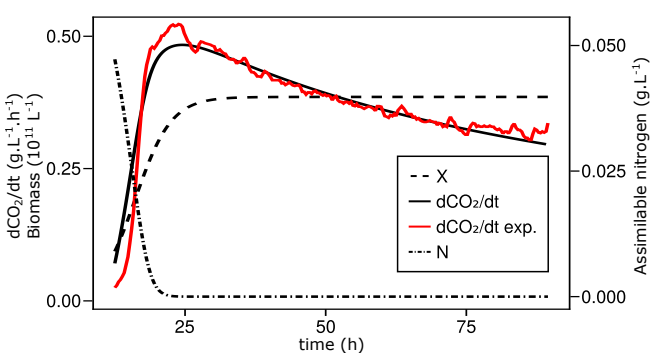

Fig. 3. Example of a fitted trajectory (in black) from experimental data (in red).

IV. Results

A. Implementation

Two methods were implemented to numerically solve the optimization problem (8): interior point method (see, e.g. [11]) and particle swarm optimization (see, e.g., [12]). They are denoted, respectively, IP and PSO in the results tables. In order to quantify the success of the method over a full fermentation, we propose for each numerical experiment the computation of two quantities ΔJ and $\Delta\xi$. For given true initial state ξ_0, measured output $\mathbf{y}$ over $[0, T]$, estimated initial state $\hat{\xi}_0$ and generated output $\hat{y}$, we define $\Delta J := \|\mathbf{y} - \hat{y}\|_{L^2(0,T)} / \|\mathbf{y}\|_{L^2(0,T)}$ and $\Delta\xi := \sup_{i \in \{1,2,3\}} |(\xi_0 - \hat{\xi}_0)_i| / |(\xi_0)_i|$. This allows to obtain a relative estimation error. See Figure IV-A for an illustration of the estimation algorithm.

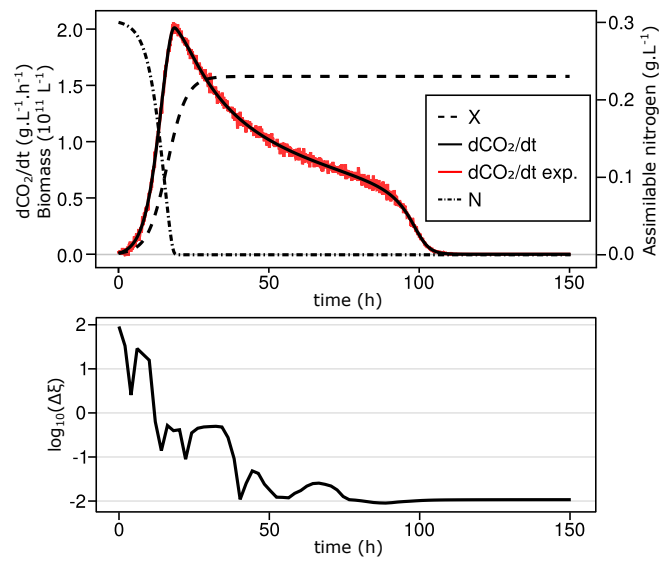

Fig. 4. Simulated online estimation using MHE. In this case, the simulated output y has been noised in order to match the experimental setting. At the top, original trajectory and noised data. At the bottom, relative error of the estimator $\Delta\xi$ for the time interval $[0, t]$ at each t. The estimation method reaches a 5% error before the 50 hours mark, well before nitrogen addition occurs.

For each method, we experimented with the estimation strategy over multiple data sets corresponding to three cases. First, we applied the estimation method to trajectories generated from the dynamical model, with 30 randomly selected initial conditions. These experiments correspond to the "0% noise" row in the result tables. The second case corresponds to noisy output: for a given ξ_0 and the associated output y, we assume that the measured output fed to the algorithm is $\mathbf{y} = (1 + \varepsilon/10)y$, where ε is a random unit Gaussian noise, also with 30 randomly selected initial conditions. These experiments correspond to the "10% noise" row in the result tables. Finally, we implemented the algorithm on 15 experimental CO_2 production measurements (see section II-B). In each of these cases, we give the mean values for ΔJ and $\Delta\xi$, as well as their standard deviation. See Table I. The same exercise, in the same conditions, has been done focusing on the partially initialized model of Section III-A. See the results in Table II.

B. Discussion of the results

We discuss the results shown in tables I and II. Let us focus first on the simulated data. Simulations agree with the theory:

Method	Data	ΔJ		$\Delta\xi$	
		Mean	Std	Mean	Std
IP	0% noise	0.0054	0.019	0.21	0.91
	10% noise	0.10	0.00062	0.024	0.040
	Experiments	0.015	0.015	7.88	7.88
PSO	0% noise	0.059	0.051	21.02	89.05
	10% noise	0.11	0.015	6.25	9.88
	Experiments	0.019	0.016	98.35	246.54

TABLE I

Method	Data	ΔJ		$\Delta\xi$	
		Mean	Std	Mean	Std
IP	0% noise	0.0011	0.0013	0.017	0.031
	10% noise	0.10	0.00047	0.022	0.029
	Experiments	0.017	0.015	7.37	7.84
PSO	0% noise	0.019	0.015	0.53	0.97
	10% noise	0.10	0.0056	0.45	0.70
	Experiments	0.087	0.29	6.62	6.65

TABLE II

AVERAGE FINAL PERFORMANCE OF THE ESTIMATOR FOR THE MALHERBE ET AL. MODEL (TABLE I) AND THE PARTIALLY INITIALIZED MODEL (TABLE II).

it is possible to fit the curve with a trajectory of the model (with ΔJ low) and to extract from it a approximate value of ξ_0 that is faithful (with $\Delta\xi$ low). If the J minimization fails, results are naturally poor for the state estimation. A 10% noise is much more intense than what is seen experimentally but serves as an illustration. Having $\Delta J = 0.1$ in particular illustrates that the noise was eliminated well.

On the topic of the optimization method, the interior point method yields much better performance. This reflects the low selectivity of the energy that is being minimized. The results of the PSO method are substantially improved in the partially initialized case (the margin of improvement for the IP method is much smaller). This suggests that introducing the new partially linearized model offers a form of robustness that allows for a weaker optimization method to still be efficient. Since the optimization problem does not appear to be highly sensitive to variations in ξ_0, ΔJ can be made low without having $\Delta\xi$ low, even in the numerical cases. Increasing the precision of the output estimation (lowering ΔJ as much as possible) is paramount to the success of the state estimation. As illustrated in the partially-linearized case, the refinement provided by the model can yield significant improvement to the state estimation.

The situation is not as clear in the case of real data. On the one hand, the minimization of the least squares energy reaches suitable levels. This can be explained by the fact that the measured output is not very noisy, as can be seen from Figures 3 and 5 (Figure 3 shows a derivative of the noisy measurement). For instance, as illustrated in Figure IV-A, such a low level of noise can lead to a quite precise estimate of the initial state (with a $\Delta\xi$ of 0.01, that is a 1% error in initial state estimation with a simulated output). However, as it clearly appears in the tables, the good fitting of the output measurement does not translate into a good estimation of the initial state.

We identify three elements in the method that may explain this discrepancy. First, the low selectivity of the least-squares energy can lead to wrong estimations of the initial state. For instance, X_0 can be drastically changed from a shift in the starting time of the experiment. This has been taken into account when possible, but does not correct the discrepancy with simulated data. Second, the parameter values in [2] have been re-fitted to better match the experimental data in our possession. As can be seen in Figure 5, the trajectory generated by the Malherbe et al. model using an experimentally measured initial state does not yield an output that is closely matched with our experimental measurements. A tighter fitting of the model would be necessary to allow the method to properly predict the initial state. Third, the model at hand may be refined, and has seen some revisions since it was proposed. We suspect that the model may have some shortcomings for this particular type of estimation problem, such as the initial state appearing as a parameter in the dynamics. This impacts the possible strategies for estimation methods. In this sense, we wish to explore the method for other more recent and better fitted models (see, e.g., [13], [14]).

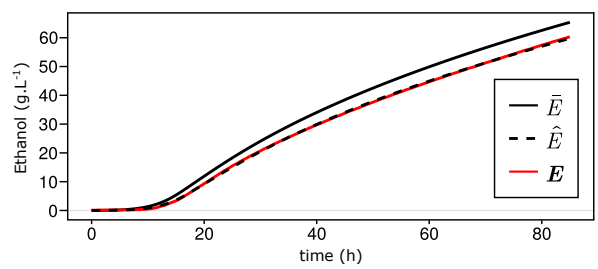

Fig. 5. Example of wrongly fitted data. The red curve ($\mathbf{E}$) corresponds to experimentally gathered data, the plain black curve is the model prediction ($\bar{E}$), and the dashed black curve ($\hat{E}$) is the fitted curve. Under the current tuning of the model, it may fail to predict the trajectory from initial conditions, even if the estimator is able to recover a fitting trajectory.

V. CONCLUSION

In this paper, we discussed a state estimation problem for alcoholic fermentation process under biogas production measurements. Based on a classical model, we showed the observability of the dynamics when endowed with that measurement. We also proposed variations on the model that may be adapted to more specific experimental scenarios. Motivated by the slow process time, we proposed to tackle the estimation task with an optimization-based moving horizon method. The technique was implemented on both numerical and experimental data. This showed that the technique allows to recover the state of the fermentation, but is beholden to the quality of the model. Our results show that the method is well adapted to the estimation problem, and so the way forward for us is to focus on more recent models, which

in particular should be better suited to the process control objectives.

Appendix I
Observability analysis

We give a full proof of well-posedness and asymptotic behavior of solutions to the problem only for model (1)-(4). The proof can be easily adapted to the other cases.

Proposition 6: Let $(S_0, N_0, X_0) \in \Omega_0 \setminus \{(0,0,0)\}$. Under isothermal conditions, letting (S, N, X, E) be the solution of (1)-(4) with initial condition $(S_0, N_0, X_0, 0)$, we have

1) $t \mapsto (S(t), N(t), X(t), E(t))$ is continuous over $[0, +\infty)$, analytic over $(0, +\infty)$.
2) S, N, X and E are positive and monotonous.
3) As $t \to +\infty$, $(S, N, X, E \to (0, 0, X_{\max}(N_0), \mu S_0)$.

Proof: First, it should be noted that the dependence of X to N_0 is non-standard for the application of ODE solutions existence theorems. We must assume that there exists N_0' a second constant and that the trajectory of X is actually that of a logistic curve with asymptote $X = X_{\max}(N_0')$. Once existence results are proved, we can freely assume that we are on the specific trajectory $N_0' = N_0$.

Regarding existence of solutions, the right-hand-side (RHS) of Equations (1)-(4) is Lipschitz continuous with respect to S, N, and X on Ω. It is, however, only locally Lipschitz continuous with respect to E on $[0, +\infty)$ (because of the non-integer power of E in ν_S, ν_N). This allows to define solutions on the time interval $[0, \varepsilon)$ for some $\varepsilon > 0$. It is clear that the RHS of (1)-(4) is actually analytic with respect to (S, N, X, E) once $E > 0$. Since $\dot{E}(0) > 0$, we assume that it is the case on $(0, \varepsilon')$ for some $\varepsilon' \leq \varepsilon$. This allows to prove the solution to (1)-(4) is analytic on $(0, \varepsilon')$.

We can now assume that we are in the case $N_0' = N_0$ and check that solutions remain in Ω_0. With $\xi = (S, N, X)$, it is easy to check that (1)-(4) translates to $\dot{\xi} = D(\xi, E(t))\xi$, with $D : \mathbb{R}^3 \times \mathbb{R} \to \mathbb{R}^{3\times 3}$ a diagonal matrix. As a result, if there exists a point $t^* \in (0, \varepsilon')$ such that one component of ξ vanishes at t^*, all derivatives of that given component must also be 0 at t^*. Since the solution is analytic, the given component is identically 0 over $(0, \varepsilon')$, which is in contradiction with the assumption that $\xi_0 \in \Omega_0$. From that we deduce that on the whole interval of existence, $\dot{S} < 0$, $\dot{N} < 0$, $\dot{X} > 0$, $X < X_{\max}(N_0)$ (that from the logistic curve only), $E = \mu(S_0 - S)$ and thus solutions are spatially bounded. This proves that solutions must exist on the whole interval $[0, +\infty)$. Now we can notice that if we replace ξ with $\zeta = (S, N, X_{\max}(N_0) - X)$, we again $\dot{\zeta} = D'(\zeta, E(t))\zeta$, with $D' : \mathbb{R}^3 \times \mathbb{R} \to \mathbb{R}^{3\times 3}$ a diagonal matrix, with all diagonal elements negative on Ω_0. As a result, $V(S, N, X) = S^2 + N^2 + (X - X_{\max}(N_0))^2$ is a strict Lyapunov function for the dynamics of ζ, proving the convergence $(S, N, X) \to (0, 0, X_{\max}(N_0))$. Convergence of E to μS_0 then follows. ■

Proof of Proposition 1: Since $t \mapsto E(t)$ and $t \mapsto \tilde{E}(t)$ are both analytic, having $E_{|[t_1,t_2]} \equiv \tilde{E}_{|[t_1,t_2]}$, with $0 \leq t_1 < t_2$ implies $E \equiv \tilde{E}$ over $[0, +\infty)$ (we include 0 since E is continuous). Since $E = \mu(S_0 - S)$ and $S(t) \to 0$, it follows that $S_0 = \tilde{S}_0$, and $S \equiv \tilde{S}$ over $[0, +\infty)$. Then from the derivative of S, we get

$$X N_{ST}(N_0 - N, X, T) = \tilde{X} N_{ST}(\tilde{N}_0 - \tilde{N}, \tilde{X}, T)$$

over $[0, +\infty)$. Passing to the limit $t \to 0$ yields $X_0 N_{ST}(0, X_0, T) = \tilde{X}_0 N_{ST}(0, \tilde{X}_0, T)$, that is $X_0 = \tilde{X}_0$. Likewise, taking $t \to +\infty$ then yields $N_0 = \tilde{N}_0$. ■

A small amendment to this proof yields Proposition 2.

Proof of Proposition 2: Points 1 and 3 of proposition 6 still holds when $S = S^{\exp} + S^{\text{lin}}$, so that $S^{\exp} \to 0$, $S^{\text{lin}} \to 0$. Point 2 holds in the sense that neither $S^{\exp}$ nor S^{lin} vanish at any point (the proof by analyticity is the same), however it may happen that $S = S^{\exp} + S^{\text{lin}}$ vanishes, as $S^{\text{lin}}(0)$ can be negative. If $E_{|[t_1,t_2]} \equiv \tilde{E}_{|[t_1,t_2]}$, with $0 \leq t_1 < t_2$, are the outputs of two trajectories of system (5)-(6)-(2)-(4), analyticity implies $E \equiv \tilde{E}$ over $[0, +\infty)$ and like in the proof of Proposition 1, we deduce that $S_0 = \tilde{S}_0$. Here $S_0 = S_0^{\exp} + S_0^{\text{lin}}$ and $S_0 = S_0^{\exp} + \tilde{S}_0^{\text{lin}}$, so $S_0^{\text{lin}} = \tilde{S}_0^{\text{lin}}$. As a consequence $S = \tilde{S}$ and the conclusion follows the same path as proof of Proposition 1. ■

References

[1] S. L. Forbes, D. A. Cohen, R. Cullen, S. D. Wratten, and J. Fountain, "Consumer attitudes regarding environmentally sustainable wine: an exploratory study of the new zealand marketplace," *Journal of cleaner production*, vol. 17, no. 13, pp. 1195–1199, 2009.

[2] S. Malherbe, V. Fromion, N. Hilgert, and J.-M. Sablayrolles, "Modeling the effects of assimilable nitrogen and temperature on fermentation kinetics in enological conditions," *Biotechnology and bioengineering*, vol. 86, no. 3, pp. 261–272, 2004.

[3] M. Soroush, "State and parameter estimations and their applications in process control," *Computers & Chemical Engineering*, vol. 23, pp. 229–245, Dec. 1998.

[4] D. Dochain, ed., *Automatic Control of Bioprocesses*. Control systems, robotics and manufacturing series, London, England: ISTE Ltd and John Wiley & Sons, June 2008.

[5] J. B. Rawlings and L. Ji, "Optimization-based state estimation: Current status and some new results," *Journal of Process Control*, vol. 22, pp. 1439–1444, Sept. 2012.

[6] J. B. Rawlings, M. M. Diehl, and D. Q. Mayne, *Model predictive control: Theory, computation and design*. Nob Hill, 2017.

[7] A. Sipos, "Sustainable method using filtering techniques for a fermentation process state estimation," *Sustainability*, vol. 12, no. 17, p. 7105, 2020.

[8] C. Fernández, N. Pantano, F. Rossomando, A. Amicarelli, and G. Scaglia, "Fermentation monitoring by bayesian states estimators. application to red wines elaboration," *Control Engineering Practice*, vol. 103, p. 104608, 2020.

[9] N. El Haloui, D. Picque, and G. Corrieu, "Alcoholic fermentation in winemaking: On-line measurement of density and carbon dioxide evolution," *Journal of Food Engineering*, vol. 8, no. 1, pp. 17–30, 1988.

[10] G. Besançon, *Nonlinear Observers and Applications*. Springer Berlin Heidelberg, 2007.

[11] A. S. Nemirovski and M. J. Todd, "Interior-point methods for optimization," *Acta Numerica*, vol. 17, p. 191–234, 2008.

[12] Z.-H. Zhan, J. Zhang, Y. Li, and H. S.-H. Chung, "Adaptive particle swarm optimization," *IEEE Transactions on Systems, Man, and Cybernetics, Part B (Cybernetics)*, vol. 39, no. 6, pp. 1362–1381, 2009.

[13] F. Beaudeau, C. A. Aceves-Lara, J. Godilllot, J.-R. Mouret, I.-C. Trelea, and C. Bideaux, "Modelling the effects of assimilable nitrogen addition on fermentation in oenological conditions," *Bioprocess and Biosystems Engineering*, vol. 46, pp. 941–955, Apr. 2023.

[14] A. G. Yabo and C. Casenave, "Aroma synthesis and energy consumption in wine fermentation: a multiobjective optimization approach," *IFAC-PapersOnLine*, vol. 56, no. 2, pp. 6211–6216, 2023.